Electronic Supplementary Material (ESI) for Lab on a Chip.

Surface acoustic wave-driven pumpless flow for sperm rheotaxis analysis

Junyang Gai[1], Citsabehsan Devendran[1], Adrian Neild[1,*], and Reza Nosrati[1,*]

[1] Department of Mechanical and Aerospace Engineering, Monash University, Clayton, Victoria 3800, Australia

* Corresponding authors:
Department of Mechanical and Aerospace Engineering, Monash University, Clayton, Victoria 3800, Australia
Emails: Reza.Nosrati@monash.edu (R.N.); Adrian.Neild@monash.edu (A.N.)
Phone numbers: +61 3 990 53627; +61 3 990 54655

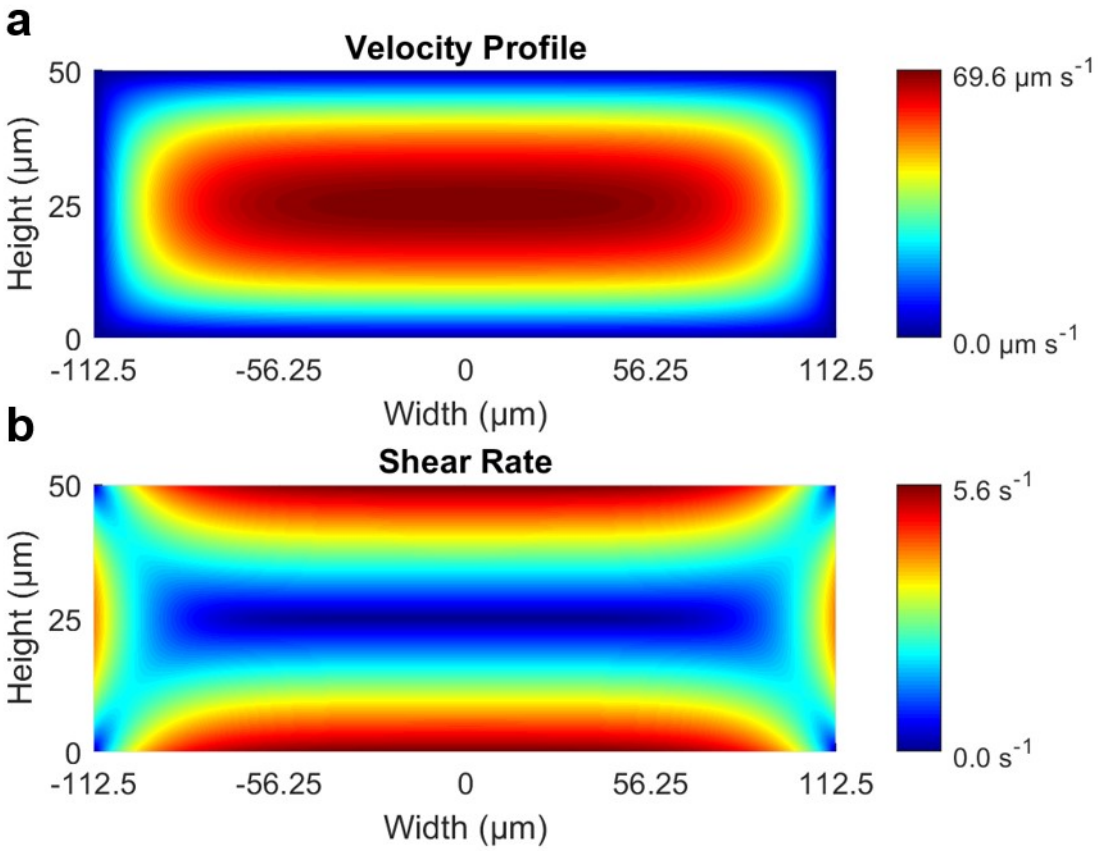

Figure S1. (a) Flow velocity and (b) shear rate profiles in the cross- sectional area of 225 μm microchannels at the average velocity of 40μm s^{-1}.

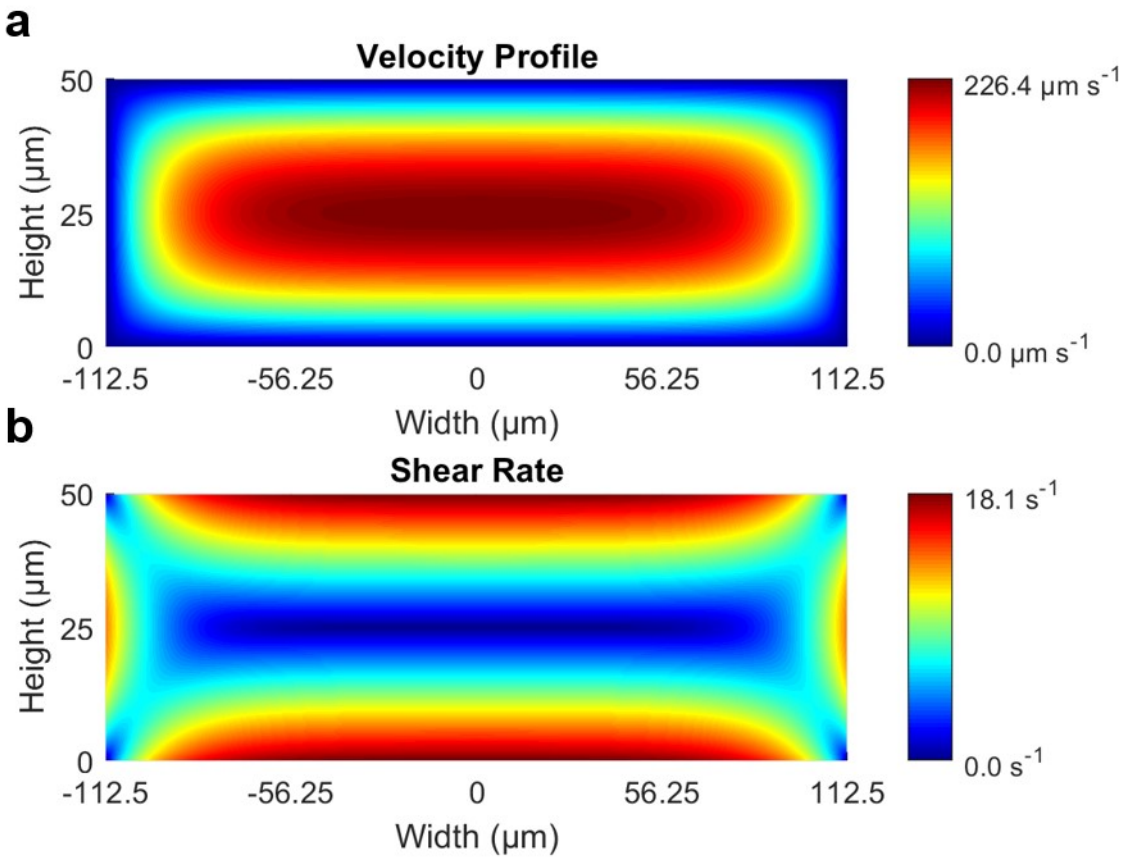

Figure S2. (a) Flow velocity and (b) shear rate profiles in the cross- sectional area of 225 µm microchannels at the average velocity of 130µm s^{-1}.

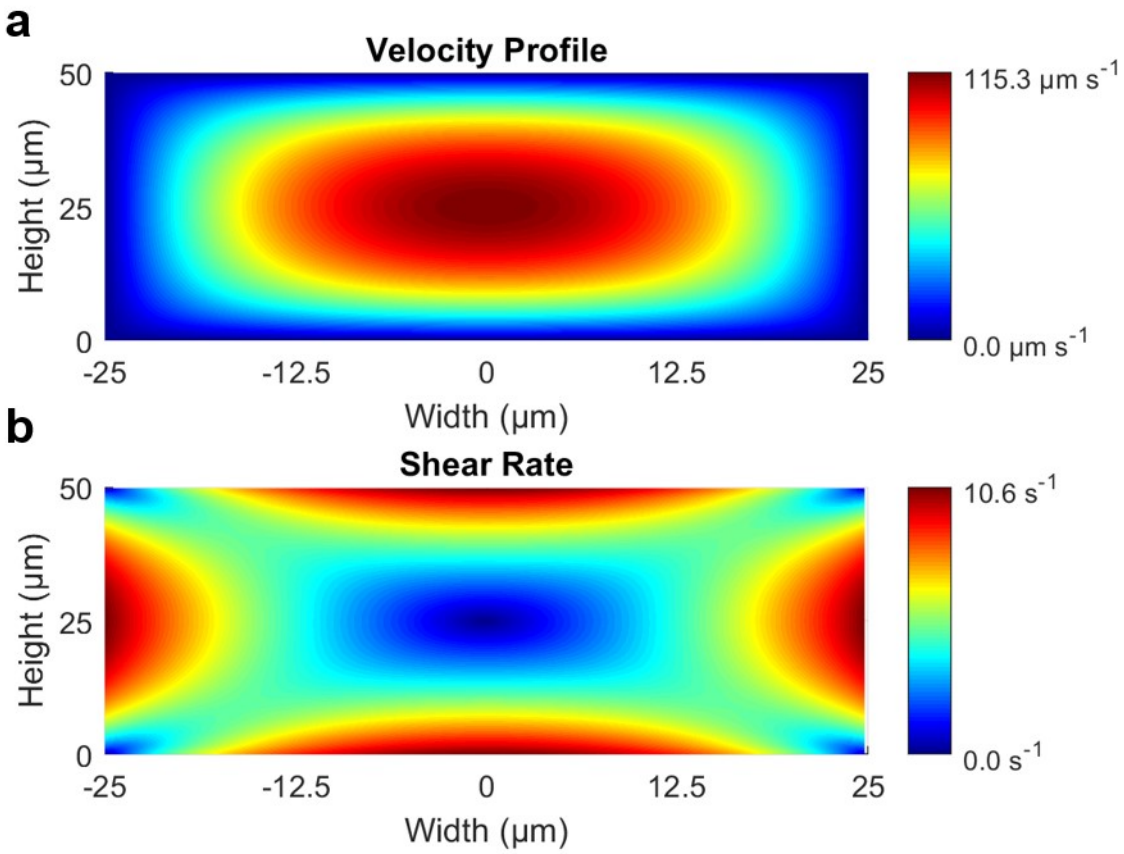

Figure S3. (a) Flow velocity and (b) shear rate profiles in the cross- sectional area of 50 µm microchannels at the average velocity of 55µm s^{-1}.

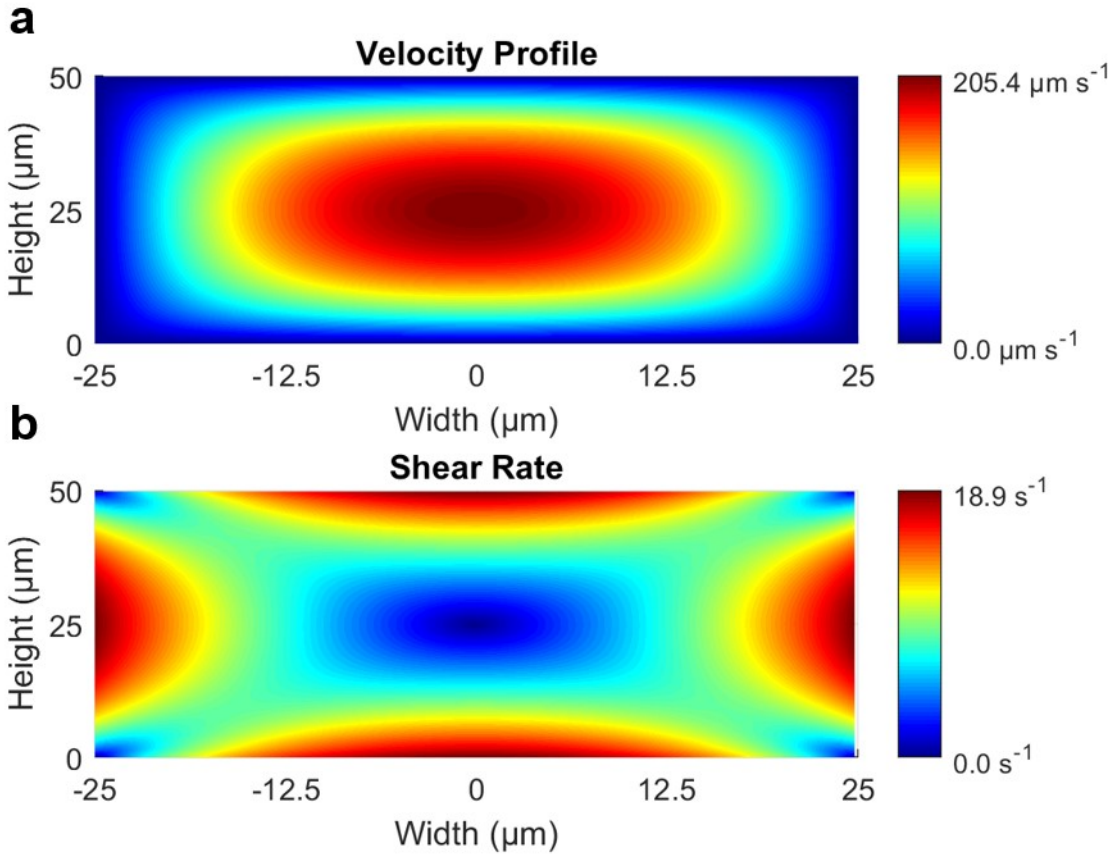

Figure S4. (a) Flow velocity and (b) shear rate profiles in the cross- sectional area of 50 μm microchannels at the average velocity of 98μm s^{-1}.

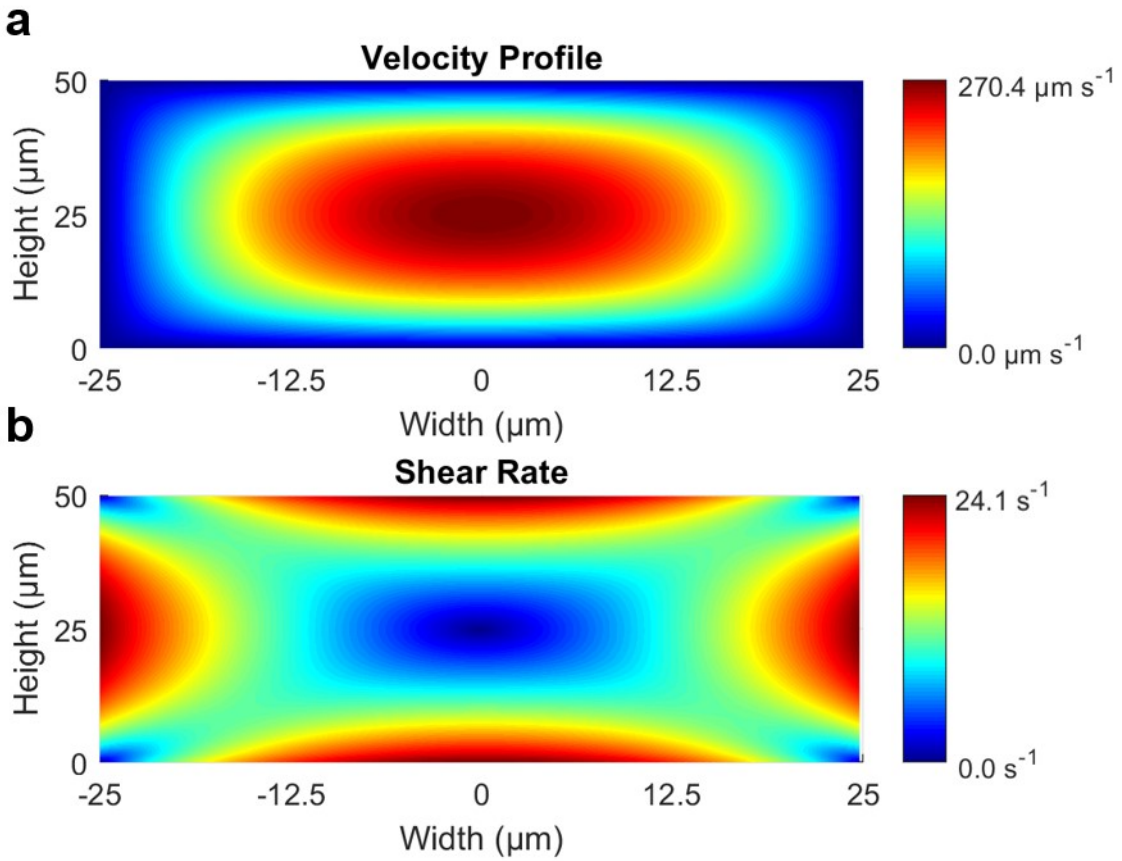

Figure S5. (a) Flow velocity and (b) shear rate profiles in the cross- sectional area of 50 μm microchannels at the average velocity of 128 μm s^{-1}.

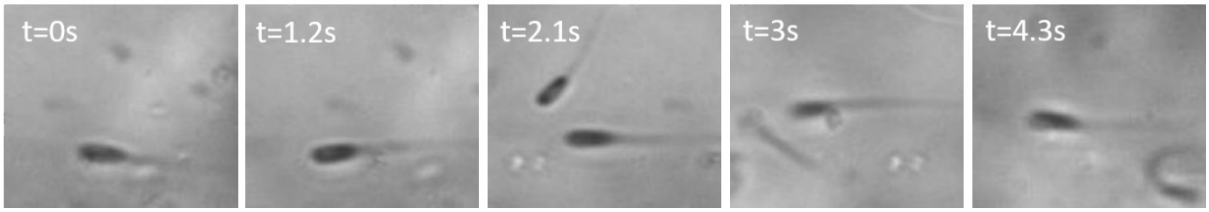

Figure S6. Representative time-lapsed images of sperm oriented parallel to the flow.

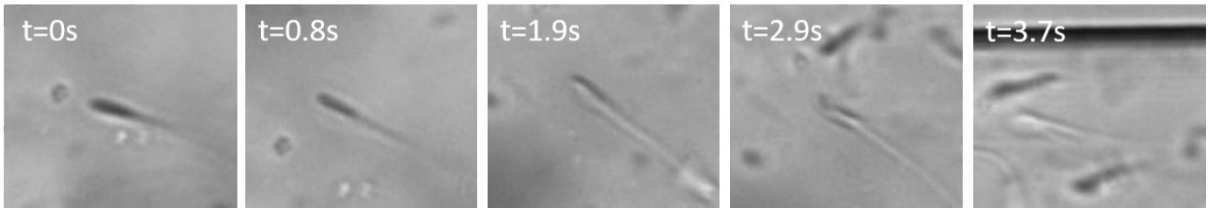

Figure S7. Representative time-lapsed images of sperm oriented tilted to the flow.

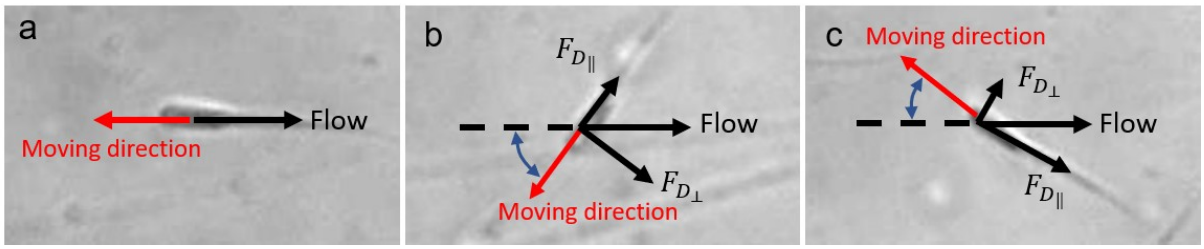

Figure S8. Representative (a) straight rheotaxis sperm (b) left-turning rheotaxis sperm, and (c) right-turning rheotaxis sperm alignment direction with respect to the flow direction. Black arrow, red arrow, and blue arrow specify flow direction, sperm moving direction, and sperm orientation angle.

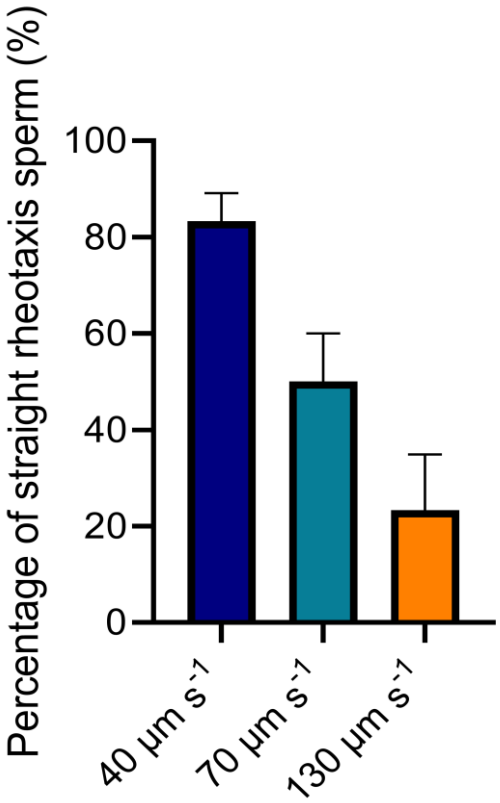

Figure S9. Percentage of sperm oriented parallel to the flow in 225-µm-wide microchannels in a flow field with an average velocity of (a) 40 µm s^{-1}, (b) 70 µm s^{-1} and (c) 130 µm s^{-1}.

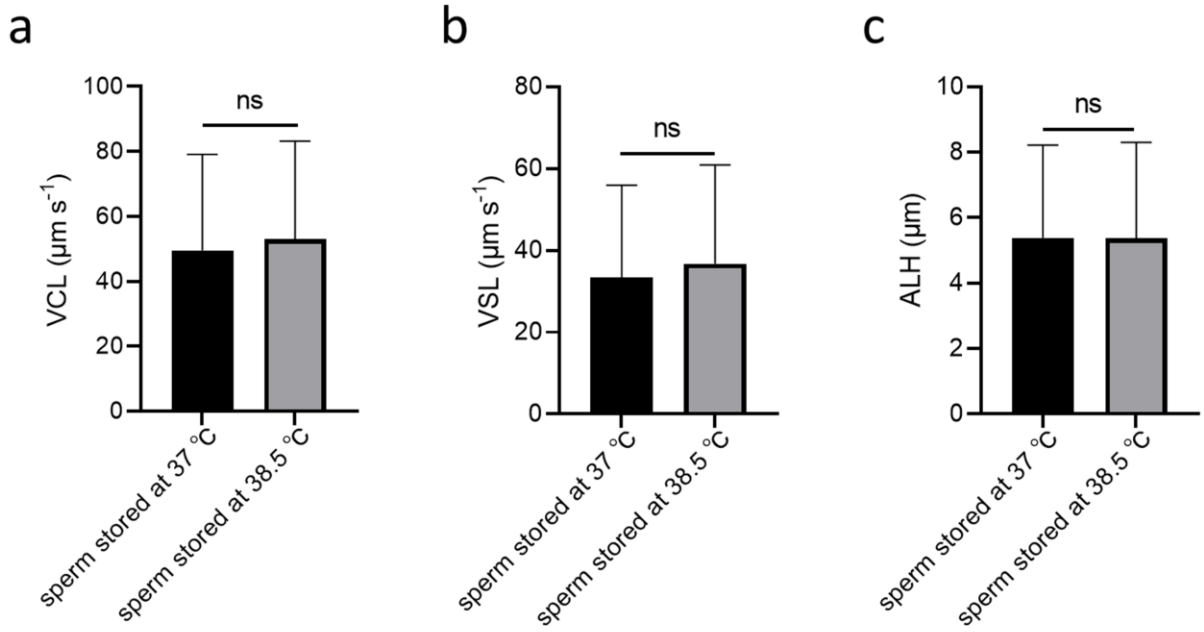

Figure S10. Comparison of (a) Curvilinear velocity (VCL), (b) Average path velocity (VAP) and (c) Lateral head displacement (ALH) of bull sperm samples cultured at 37 ℃ and 38.5 ℃. All data represented as mean ± s.d from three independent experiments peformed using different samples. *p*-values were determined by unpaired t test with welch's corrections.

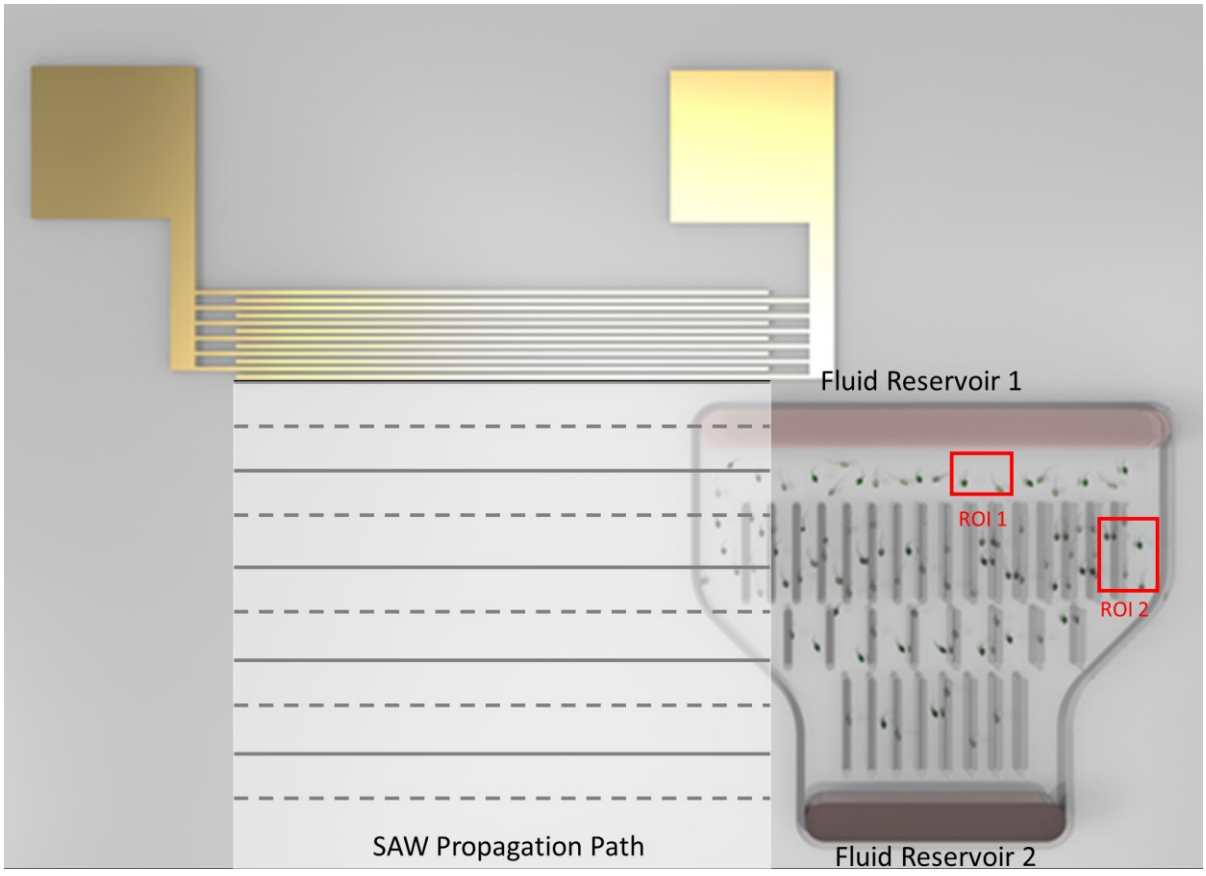

Figure S11. Relative position of the microfluidic channel and SAW propagation path.

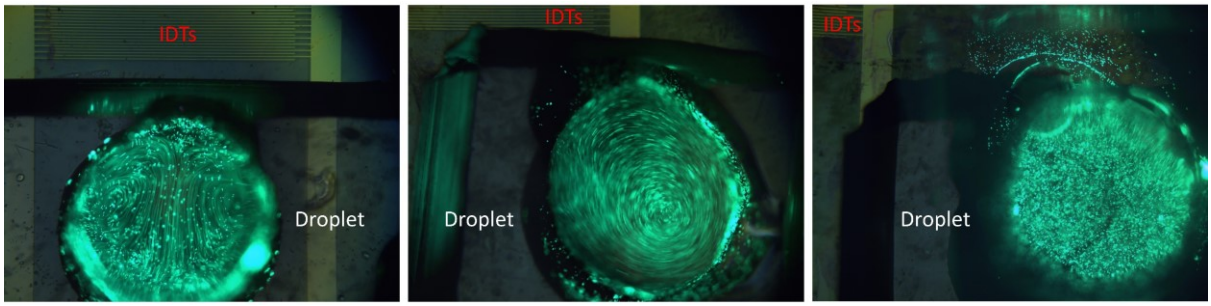

Figure S12. Acoustic streaming in the droplet (a) entirely present on SAW propagation path, (b) partially present on SAW propagation path, and (c) absent on SAW propagation path.